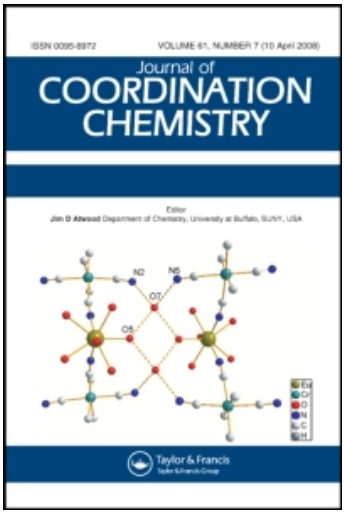

Journal of Coordination Chemistry
Publication details, including instructions for authors and subscription information:
http://www.informaworld.com/smpp/title~content=t713455674

DYNAMIC ELECTROCHEMISTRY OF CIS-$[Co(EN)_2(ENH)Cl]Cl_3 \cdot H_2O$ AND $[Co(EN)_3]Cl_3$ COMPLEXES

Michal Wilgocki[a]; Stanislaw Baczynski[a]; Maria Cyfert[a]; Edward Giera[a]; Marek Jaroszewski[a]
[a] Institute of Chemistry, University of Wroclaw, Wroclaw, Poland

To cite this Article Wilgocki, Michal , Baczynski, Stanislaw , Cyfert, Maria , Giera, Edward and Jaroszewski, Marek(1995) 'DYNAMIC ELECTROCHEMISTRY OF CIS-$[Co(EN)_2(ENH)Cl]Cl_3 \cdot H_2O$ AND $[Co(EN)_3]Cl_3$ COMPLEXES', Journal of Coordination Chemistry, 34: 2, 99 — 117
To link to this Article: DOI: 10.1080/00958979508055390
URL: http://dx.doi.org/10.1080/00958979508055390

J. Coord. Chem., 1995, Vol 34, pp. 99–117
Reprints available directly from the publisher
Photocopying permitted by license only

DYNAMIC ELECTROCHEMISTRY OF CIS-$[Co(EN)_2(ENH)Cl]Cl_3 \cdot H_2O$ AND $[Co(EN)_3]Cl_3$ COMPLEXES

MICHAL WILGOCKI,* STANISLAW BACZYNSKI, MARIA CYFERT, EDWARD GIERA and MAREK JAROSZEWSKI

Institute of Chemistry, University of Wroclaw, F. Joliot-Curie 14, 50–383 Wroclaw, Poland

(Received July 19, 1994)

The polarographic and voltammetric behaviour of *cis*-$[Co(en)_2(enH)Cl]Cl_3 \cdot H_2O$ and $[Co(en)_3]Cl_3$ in water and dimethylsulphoxide has been investigated at a dropping mercury electrode, a hanging mercury drop electrode and a Pt planar electrode. The ECE mechanism for electrochemical conversion of the protonated, partly-chelated *cis*-$[Co(en)_2(enH)Cl]^{3+}$ complex into $[Co(en)_3]^{3+}$ was established on the basis of dynamic electrochemistry investigations. For the second step of the reduction, $[Co(en)_3enH]^{3+}$ to Co(Hg), the electrode reaction mechanism varies with changes in the degree of complexation. Reduction of Co(II) in ethanediamine/2-aminoethylammonium buffer solution in the presence of a small amount of human blood serum at nearly neutral pH is catalytic in nature.

KEYWORDS: *cis*-Chloro*bis*(1,2-ethanediamine) (2-aminoethylammonium)cobalt(III) Chloride, *tris*(1,2-ethanediamine)cobalt(III) Chloride, dynamic electrochemistry, electrode reaction mechanism

INTRODUCTION

The octahedral, totally chelated $[Co(en)_3]Cl_3$ complex was first prepared by Jørgensen in 1989.[1] The first inert complex containing 2-aminoethylammonium cation (enH^+) as a monodentate ligand, $[Cr(en)(enH)Cl_3]$, was isolated in solid state by Werner in 1916.[2] To our knowledge over a dozen protonated (partly- and non-chelated) ethanediamine-metal ion complexes have been isolated in the solid state,‡ among them *cis*-$[Co(en)_2(enH)Cl]Cl_3 \cdot H_2O$.[7]

* Author for correspondence.

‡The following protonated (partly- and non-chelated) ethanediamine-metal ion complexes have been isolated in the solid state: $[Cr(en)(enH)Cl_3]Cl$,[2] $[Pd(en)(enH)Cl]PdCl_4$,[3] $[Pd(en)(enH)Cl]Cl_2 \cdot H_2O$,[3] $[Pt(enH)_2Cl_2]Cl_2$,[4] $[Pt(enH)(NH_3)Cl_2]Cl$,[4] $[Co(en)(enH)Cl_3]Cl$,[5] $[(NH_3)_5Cr\text{-}OH\text{-}Cr(NH_3)_4(enH)]^{6+}$,[6] *cis*-$[Co(en)_2(enH)Cl]Cl_3 \cdot H_2O$,[7] $Na_2[Fe(CN)_5(enH)] \cdot H_2O$,[8] *cis*-$[Rh(en)_2(enH)Cl]Cl_3 \cdot 2H_2O$,[9] *cis*-$[Ru(en)_2(enH)Cl]Cl_3$,[10] *cis*-$[Ru(en)_2(enH)Cl]Cl \cdot ZnCl_4$,[10] *mer*-$[Ir(en)(enH)Cl_3]Cl \cdot H_2O$,[11] $[Pt(enH)Cl_5] \cdot H_2O$,[12] $[Pt(enH)Cl_3]$,[13]. The non-protonated, partly-chelated, *mer*-$[Ir(en)(en^*)Cl_3]$, complex has also been isolated in the solid state[14] (en^* denotes a monodentate ethanediamine molecule). Recently, the crystal structures of the $[Pt(enH)Cl_5] \cdot H_2O$,[12] $[Pt(enH)Cl_3]$,[13] *mer*-$[Ir(en)(enH)Cl_3]Cl \cdot H_2O$,[14] *mer*-$[Ir(en)(en^*)Cl_3]$ complexes[14] have been determined. Several protonated ethanediamine – metal ion complexes have been studied in aqueous solution or have been proposed as intermediate species in reaction rate studies of the acid hydrolysis of both inert[15–25,28,30] and labile complexes.[26,27,29,31]

Electrochemistry of inert, protonated ethanediamine — metal ion complexes, however, has received little attention. Only Matsubara and Ford[10] have used cyclic voltammetry for characterization (estimation of the formal potential) of *cis*-$[Ru\text{-}(en)_2(enH)Cl]^{3+}$ and $[Ru(en)_2(enH)(H_2O)]^{4+}$ (obtained by photolysis of $[Ru(en)_3]^{3+}$). No electrochemistry of *cis*-$[Co(en)_2(enH)Cl]^{3+}$ has been reported. The contrary is the case with $[Co(en)_3]Cl_3$, which has been studied by several authors.[32–39] Bjerrum[32] showed that the stability constant of $[Co(en)_3]^{3+}$ could be determined from measurements of redox potentials of the $[Co(en)_3]^{3+}/[Co(en)_3]^{2+}$ system at sufficient excess of equilibrium ethanediamine concentration. Konrad and Vlček[35] have proven that $[Co(en)_3]^{2+}$ is the only electroactive species in the polarographic oxidation of the Co(II)-en system at the dropping mercury electrode. Ito has reported[36] the catalytic nature of polarographic reduction of the $[Co(en)_3]^{3+}$ – protein = (egg albumin, β-amylase, egg lysozyme)] system in ammonia buffers. Fischerova, Dračka and Meloun[40] have established the ECE mechanism for the polarographic reduction of *cis*- and *trans*-$[Co(en)_2Cl_2]^+$ in the presence of ethanediamine. It was also shown electrochemically[41–47] that in the totally labile Zn(II)-, Cd(II)-, Hg-(II)-en–3M $(Na,H)ClO_4$ system, protonated non- and partly-chelated ethanediamine complexes coexist in equilibrium with chelated complexes.

In this paper, we present the dynamic electrochemistry of *cis*-$[Co(en)_2(enH)Cl]^{3+}$ with respect to $[Co(en)_3]^{3+}$ at mercury and platinum electrodes in aqueous and DMSO solution. The main aim of the study was to elucidate the electrode reaction mechanism for the reduction of *cis*-$[Co(en)_2(enH)Cl]^{3+}$. Both for oxidation and reduction, respectively, of the Co(II)-en-enH^+ and Co(II)-en-enH^+-human blood serum systems, variations in electrode reaction mechanism with changes in complexation are revealed. The necessity of taking into account the protonated, non- and partly-chelated $[Co(en)_i(enH)_j]^{(2+j)+}$ species is demonstrated. The limitations of electrochemical methods for deducing the details of the electrode reaction mechanism for the title complex and for the Co(II)-en-enH^+ and Co(II)-en-enH^+-human blood serum systems have also been discussed.

EXPERIMENTAL

Syntheses of $Co(en)_3Cl_3$ and *cis*-$[Co(en)_2(enH)Cl]Cl_3 \cdot H_2O$ were performed according to literature procedures[7,48] using chemicals of the highest purity commonly available. The complexes were characterized as described in Ref. 7. Triply distilled water and freshly distilled (5A molecular sieve, under argon) dimethylsulfoxide, DMSO (for UV-Spectroscopy, Fluka), were used as solvents; 1,2-ethanediamine, en (puriss., p.a., Fluka) was redistilled before use. The concentration of stock 1,2-ethanediamine solution was determined by titration with standard $HClO_4$ solution. 1,2-ethanediammonium diperchlorate and dichloride, $enH_2(ClO_4)_2$, enH_2Cl_2, were synthesized as previously described.[44] The concentration of stock $NaClO_4$ (G.R. Merck) solution was determined by titration of the eluate from a cation-exchange column with standard NaOH solution. The concentration of KCl (puriss., p.a., POCH Gliwice) stock solution, was determined by mercurimetric titrations using $Na_2[Fe(CN)_5NO]$ as indicator.[49] Tetrabutylammonium perchlorate, TBAP, was prepared from tetrabutylammonium

hydroxide (40% in water, pract., Fluka) by adding $HClO_4$ solution. The TBAP obtained was recrystallized from ethanol and dried under vacuum prior to use.

DC polarographic measurements with a dropping mercury electrode (DME) were perfomed by means of a Redelkis OH-105 polarograph. Voltammetric and cyclic voltammetric studies were carried out on Laboratorni Pristroje Polarographic Analyser (PA3 and PA4) for slow scan rates (vs $\leq$ 0.2V/s) and on a Telpod (Poland) Digiscope Polarograph (type OP-5) for moderately fast scan rates ($0.3 \leq v \leq 40$V/s). Preliminary i-E curves were recorded using an XY recorder (Laboratorni Pristroje, type 4103 and 4106) for slow scan rates (with PA3 and PA4) and on the monitor screen (with OP-5) for scan rates faster than 0.2 V/s. The final voltammetric curves (single and repetitive) were collected using a measuring system consisting of a PA3 and PA4 and an OP-5 potentiostat connected to an IBM PC computer *via* an Ambex (Poland) AC module, type LC-020. The i-E data were elaborated using a program written in our laboratory. Two indicator electrodes were used in voltammetric measurements: a Pt planar electrode (home made) or a hanging Hg drop electrode (HMDE) of a Laboratorni Pristroje type SMDE 1, respectively. The polarographic and voltammetric cells were closed jacketted vessels (with a thermostatted water flow), provided with the respective indicating electrode, Luggin capillary, salt bridge, reference (Hg/Hg_2Cl_2, satd. NaCl) electrode, Pt spiral auxiliary electrode, a side arm for introducing deoxygenated test solution (under argon pressure), and a glass tube for argon inlet and outlet.[50]

The controlled potential coulometric and spectroelectrochemical measurements were carried out with a Radelkis OH 404A potentiostat connected with an OH 404C digital integrator unit and an HP 8452A Diode Array Spectrophotometer or Radiopan ESR (Poland). The coulometric (0.5–2 cm^3) and spectroelectrochemical (0.25 mm — thick thin-layer (UV-VIS), 0.2 cm^3 (*in situ* ESR)) cells were provided with a platinum gauze or mercury pool (coulometry) or platinum minigrid (Pt-Ir10%, 225 mesh; UV-VIS-) or hanging Pt drop (ESR-spectroelectrochemistry) working electrode, a platinum auxiliary electrode, and a reference electrode (SCE) with a micro-salt bridge (J-shaped quartz Luggin capillary). The cathodic and anodic compartments of the coulometric cells were separated by a fine porosity frit and both were provided with a glass tube for argon inlet and outlet and a side arm for introducing test solution or supporting electrolyte, respectively. Glass electrode measurements were performed in a closed, jacketted vessel with thermostatted water flow. The pH ($= -\log [H^{+}]$) was measured with respect to that of standard $HClO_4$ solutions (pH = 3) using a glass electrode (Radiometer G 202 C), a Kawai reference half-cell and with an Orion Research Digital Ionanalyser (Model 701A). The temperature was maintained at 25 ± 0.1 °C. A given volume of HCl of $HClO_4$ was automatically added from an autoburette (Metrohm, Dosimat 725) and human blood serum was delivered from a calibrated microsyringe (Hamilton). The cells were deaerated by passing a stream of argon (20 min.) prior to introducing the deoxygenated test solutions. During measurements, the argon was passed over test or supporting electrolyte solution. Argon (99.995% pure) was purified by passing it consecutively through three bubblers with spiral grooved inner-tubes containing a concentrated solution of pyrogallol in 50% KOH, acid chromium(II) sulphate solution with amalgamated zinc and supporting electrolyte (($NaClO_4$, KCl, enH_2Cl_2, or $enH_2(ClO_4)_2$)/H_2O or TBAP/DMSO, respectively).

RESULTS AND DISCUSSION

Electrochemistry of cis-[Co(en)$_2$(enH)Cl]Cl$_3$·H$_2$O and [Co(en)$_3$]Cl$_3$ Complexes in Aqueous Solution at Mercury Electrodes

In aqueous solution, the same form of the voltammogram (at HMDE) or polarogram (at DME), respectively, is obtained, independent of whether the starting complex is $[Co(en)_3]Cl_3$ *or cis*-$[Co(en)_2(enH)Cl]Cl_3 \cdot H_2O$. For both complexes, two well shaped peaks (at HMDE) or waves (at DME), which correspond to the reduction of Co(III)-/Co(II)- and Co(II)-complexes/Co(Hg), are observed (besides the characteristic peak of Hg_2Cl_2/Hg). Under linear scan voltammetry and DC polarography conditions, the former ((III)/(II)) appears at a potential of about −0.45 V, while the latter ((II)/(O)) at a potential of about −1.2 V *vs* SCE (Fig. 1).

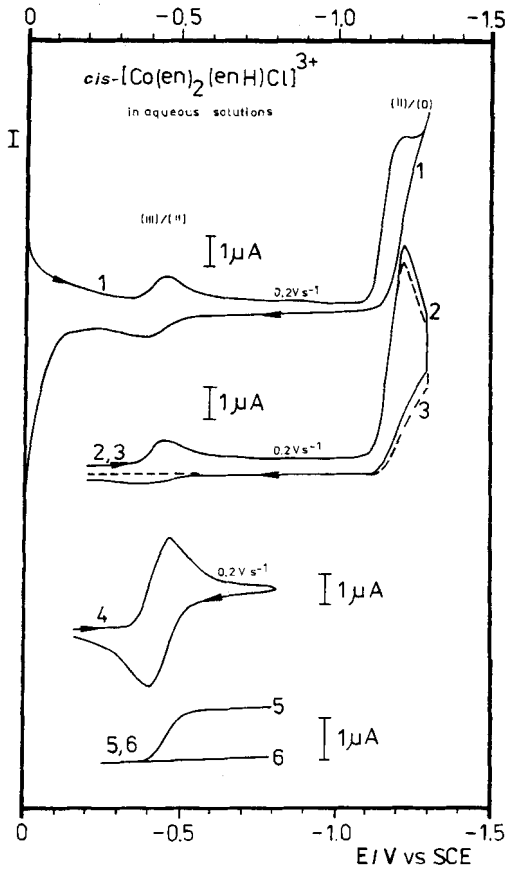

Figure 1 Cyclic voltammograms and DC polarograms of [*cis*-$[Co(en)_2(enH)Cl]Cl_3 \cdot H_2O]_o = 10^{-3}$ M in aqueous solution at 25°C, at a hanging mercury drop electrode (curve 1–4) or a dropping mercury electrode (curve 5, 6). Scan rate: 0.2 Vs^{-1} (curve 1–4), 1×10^{-3} V s^{-1} (5, 6). Drop time t_1 = 3 s (5, 6). Supporting electrolyte: $[KCl]_o$ = 1 M (curve 1); $[KCl]_o$ = 1 M, $[enH_2Cl_2]_o = 2 \times 10^{-3}$ M (curve 2); $[KCl]_o$ = 1 M, $[enH_2Cl_2]_o = 10^{-2}$ M (curve 3); $[enH_2(ClO_4)_2]_o$ = 2.436 M, pH = 7.078, $p[en]_e$ = 4.250, $p[enH^+]_e$ = 0.518, $p[enH_2^{2+}]_e$ = −0.329, (curve 4, 5, 6).

The potentials of both peaks (waves) depend on the equilibrium concentration of ethanediamine and also (to smaller degree) on the kind of supporting electrolyte (medium effect, Table 1).

Analysis of the peak and half peak potentials and logarithmic analysis of the respective DC waves shows that the first peak (wave) corresponds to the totally reversible electrode reaction (2.303RT/nF = 60 ± 1.5 mV). Cyclic voltammetry at HMDE shows that the anodic peak current value for the electrochemically reversible, one-electron electrode reaction ((III)/(II)) depends on the equilibrium ethanediamine concentration (Fig. 1, curve 2–4; Table 1). In classical supporting electrolytes ($NaClO_4$, KCl), without external addition of en, the anodic peak current of the first peak ((II)/(III)) is smaller than the respective cathodic one (Table 1). Small additions of mineral acid (*e.g.*, HCl already at concentrations approaching the concentration of the examined complex cation) leads to a strong decrease (and with further addition — to complete disappearance) of the anodic current. Similarly, small additions of the $enH_2(ClO_4)_2$ causes a decrease of i_{p_a}/i_{p_c} values (Fig. 1, curve 2, 3), while for high concentrations of $enH_2(ClO_4)_2$ (> 0.5 M) pH increase causes a decrease of the i_{p_a}/i_{p_c} ratio (curve 4 in Fig. 1). In alkaline solutions of ethanediamine (pH ≥ 10) the i_{p_a} value is equal to the i_{p_c} value (Table 1). For $[Co(en)_3]Cl_3$ as starting complex, the data obtained from bulk electrolysis with controlled potential of the mercury cathode (at $E_c^I = -0.5$ V *vs* SCE) are consistent with one-electron reduction.

For the second peak ((II)/(O)), whether the examined complex cation be $[Co(en)_2(enH)Cl]^{3+}$ or $[Co(en)_3]^{3+}$, both the current and peak potential ($E_p^{II} \simeq -1.2$ V) strongly depend on the total concentration of 1,2-ethanediammonium salt, $[enH_2X_2]_o$. At small concentrations ($[enH_2X_2]_o \simeq [Co(en)_i(enH)_jCl]_o^{3+}$) one totally irreversible peak is observed (curve 2–3 in Fig. 1). Its E_{p_c} value depends on the scan

Table 1 Cyclic voltammetric data for $Co(en)_3Cl_3$ and *cis*-$[Co(en)_2(enH)Cl]Cl_3 \cdot H_2O$ at the hanging mercury drop electrode in different supporting electrolytes at 25°C (aqueous solutions).

Complex cation	Medium	Scan rate mV/s	E_{p_c}/mV	E_{p_a}/mV	i_{p_a}/i_{p_c}	$E_f^?$/mV
$[Co(en)_3]^{3+}$	0.1 M $NaClO_4$	200	− 440[a]	− 360[a]	0.51	
	0.1 M $NaClO_4$	200	− 487[a]	− 417[a]	1.0	− 452[a]
	+ 0.574 M en	100	− 485[a]	− 420[a]	0.99	− 452.5[a]
		50	− 485[a]	− 420[a]	0.98	− 452.5[a]
		20	− 485[a]	− 420[a]	0.99	− 452.5[a]
	1 M KCl	200	− 502[b]	− 430[b]	0.67	
	1 M KCl +	200	− 550[b]	− 490[b]	1.0	− 520[b]
	0.1 M en	100	− 550[b]	− 487[b]	1.02	− 518.5[b]
		50	− 550[b]	− 485[b]	1.0	− 517.5[b]
		20	− 550[b]	− 485[b]	0.99	− 517.5
	2.463 M $enH_2(ClO_4)_2$, pH = 7.078	200	− 467[c]	− 400[c]	0.86	
cis-$[Co(en)_2(enH)Cl]^{3+}$	2.463 M $enH_2(ClO_4)_2$, pH = 7.078	200	− 468[c]	− 401[c]	0.87	
	1 M enH_2Cl_2, pH = 6.951	200	− 480[a]	− 405[a]	0.82	

[a] SCE (satd. NaCl), [b] SCE (2M KCl), [c] SCE (satd. NaCl) 11 6M $NaClO_4$, $E_f^?$ = (Epa + Epc)/2 (for ipa/ipc = 1).

rate and on complexation degree with en. In these conditions the formation of the protonated complexes in the bulk of the solution is negligibly small. However, the peak current (*c.f.*, curve 2–3 in Fig. 1) and the slope of the logarithmic analysis of the totally irreversible polarographic waves depend on the complexation degree. The voltammograms 1–3 in Figure 1 and 1–6 in Figure 2 explicitly show the variation in electrode reaction mechanism with change of complexation degree for the (II)/(O) reduction step. Especially, for high total $enH_2(ClO)_2$ concentrations and low pH (3–5), where the complexation degree is negligibly small (pH ≃ 3.5), or small (pH ≃ 5), two overlapping peaks are observed (curve 1, 2 in Fig. 2). At pH ≃ 6 the

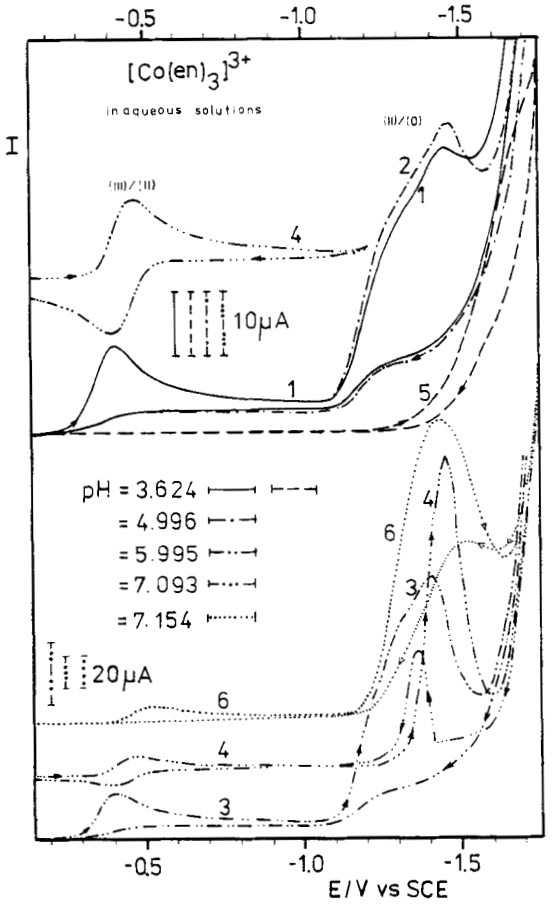

Figure 2 Cyclic voltammograms of $[[Co(en)_3]Cl_3]_o = 5 \times 10^{-3}$ M in aqueous solutions at 25°C, at a hanging mercury drop electrode. Scan rate: 0.2 V s^{-1}. $[enH_2(ClO_4)_2]_o$ = 1 M, pH = 3.624, $p[en]_e$ = 11.487, $p[enH^+]_e$ = 4.301, $p[enH_2^{2+}]_e \cong 0.000$, —— (curve 1); pH = 4.996, $p[en]_e$ = 8.744, $p[enH^+]_e$ = 2.930, $p[enH_2^{2+}]_e$ = 0.001, – · – (curve 2); pH = 5.996, $p[en]_e$ = 6.748, $p[enH^+]_e$ = 1.934, $p[enH_2^{2+}]_e$ = 0.005, – · · · (curve 3); pH = 7.093, $p[en]_e$ = 4.609, $p[enH^+]_e$ = 0.892, $p[enH_2^{2+}]_e$ = 0.060, – · · · · (curve 4). Supporting electrolyte only: $[enH_2(ClO_4)_2]_o$ = 1 M, pH = 3.624, $p[en]_e$ = 11.487, $p[enH^+]_e$ = 4.301, $p[enH_2^{2+}]_e \cong 0.000$, – – – (curve 5). $[[Co(en)_3]Cl_3]_o = 5 \cdot 10^{-3}$ M, $[enH_2(ClO_4)_2]_o$ = 1 M, pH = 7.154, $p[en]_e$ = 4.495, $p[enH^+]_e$ = 0.839, $p[enH_2^{2+}]_e$ = 0.068, 0.05% human blood serum, · · · · · (curve 6).

observed peak is the superposition of three peaks, and its total height is about twice that at pH ≃ 3.5 (curve 3 in Fig. 2). The narrow peak at pH ≃ 7 (E_{p_c} = − 1440 mV is about five times as high as that observed at pH ≃ 3.5 and has catalytic character. Under those conditions, addition of blood serum (0.005–1.0%; *c.f.*, curve 6 in Fig. 2) leads to a considerable broadening of the peak at −1440 mV. However, contrary to Brdička's solution ($[Co(NH_3)_6]Cl_3$ = 10^{-3} M, $[NH_3]$ = $[NH_4OH]$ = 0.1 M)[51] two separated waves (corresponding to the evolution of hydrogen catalysed by proteins) and preceded by the $[Co(en)_i]^{2+}$ reduction wave are not observed. On the other hand, for the Co(III)/Co (II) step, the E_{p_c} value shifts exponentially towards more negative potentials with further blood serum addition (−475 mV, 0.00% −525 mV, 0.05%; −565 mV, 0.1% −615 mV, 0.35%, −625 mV, 0.6%; −650 mV, 1.0%). Moreover, even with a small addition of blood serum (0.05%) the anodic peak for Co(II)/Co(III) step is not observed (curve 6 in Fig. 2). Addition of cysteine ($2.65 \times 10^{-5} - 5 \times 10^{-4}$ M) does not negate the reversibility of the Co(II)/Co(III) step under the same experimental conditions ($[[Co(en)_3]Cl_3$ = 10^{-3} M,$[enH_2(ClO_4)_2]$ = 1 M, pH = 7.154).

Rationalization of the Electrochemical Results for cis-*$[Co(en)_2(enH)Cl]Cl_3 \cdot H_2O$ and $[Co(en)_3]Cl_3$ in Aqueous Solution at the Mercury Electrodes*

Under voltammetric conditions at the mercury electrodes, a signal directly coming from the reduction of *cis*-$[Co(en)_2(enH)Cl]^{3+}$ is not observed. It should be noted that this complex is stable and during voltammetric studies a noticeable change in the characteristic pink colour of its aqueous solutions is not observed (even with a small addition of en). At the electrode layer, however, *cis*-$[Co(en)_2(enH)Cl]^{3+}$ transforms (even without external en addition) into relatively labile, totally chelated $[Co(en)_3]^{2+}$. A possible mechanism is characterized by the following reaction sequence:

$$cis\text{-}[Co(en)_2(enH)Cl]^{3+} + e \xrightarrow{k^{fh}_{211}} cis\text{-}[Co(en)_2(enH)Cl]^{2+}, \qquad (1)$$

where $E^{[Co(en)_2(enH)Cl]^{3+}}_{1/2} - E^{Hg_2Cl_2}_{1/2} > O$,

k^{fh}_{211} is the heterogenous electron transfer rate constant;

$$cis\text{-}[Co(en)_2(enH)Cl]^{2+} \xrightarrow{k^{-Cl^-}_{211}} cis[Co(en)_2(enH)]^{3+}_{aq} + Cl^-, \qquad (2)$$

Cl^- dissociation is very fast ($t_{1/2} < 2$ μs, c.f., Ref. 26, 27);

$$cis\text{-}[Co(en)_2(enH)]^{3+}_{aq} + H_2O \underset{k^{-H}_{21*}}{\overset{k^{-H}_{21*}}{\rightleftharpoons}} cis\text{-}[Co(en)_2(en^*)]^{2+}_{aq} + H_3O^+, \qquad (3)$$

$k^f_{21} \uparrow\downarrow k^f_{21}$ $\quad [Co(en)_2]^{2+}_{aq}$ + enH^+ $\qquad$ $k^d_{21*} \uparrow\downarrow k^f_{21*}$ $\quad [Co(en)_2]^{2+}_{aq}$ + en $\quad k^f_{30*} \uparrow\downarrow k^d_{30*}$ $[Co(en)_3]^{2+}$

where $k^{Cl^-}_{211}$, $k^{-H^+}_{21}$, $k^{+H^+}_{21}$...,k^f_{30*}, k^d_{30*} are the homogeneous rate constants,
en* denotes ethanediamine, attached as a monodentate ligand.

$[Co(en)_3]^{2+}$ formed at the electrode layer at more positive potentials than $E^\circ_{[Co(en)_3]^{3+/2+}}$, undergoes, in turn, one-electron oxidation to $[Co(en)_3]^{3+}$.

$$[Co(en)_3]^{2+} \Leftrightarrow [Co(en)_3]^{3+} + e \qquad (4)$$

Thus, if the potential was stepped from e.g., −0.15 V to −0.75 V *vs* SCE, the voltammetrically reversible peak (at −0.468 V) corresponds to the reduction of $[Co(en)_3]^{3+}$ to $[Co(en)_3]^{2+}$ (Fig. 1). On the reverse, anodic scan the coupled peak is observed (at −0.401 V) for re-oxidation of the $[Co(en)_3]^{2+}$ complex. It is only this process ($[Co(en)_3]^{3+} + e \Leftrightarrow [Co(en)_3]^{2+}$, denoted as (III)/(II) in Fig. 1), that is directly visible in voltammetric studies of *cis*-$[Co(en)_2(enH)Cl]^{3+}$ at the mercury electrodes in aqueous solutions. It should be noted that the cathodic peak current is proportional to the equilibrium concentration of $[Co(en)_3]^{3+}$ formed in the electrode layer (reaction (*4*)), and not to the concentration of *cis*-$[Co(en)_2(enH)Cl]^{3+}$ in the bulk of the solution. Therefore, the cathodic peak current obtained in the *cis*-$[Co(en)_2(enH)Cl]^{3+}$ solution is smaller than in the $[Co(en)_3]^{3+}$ (as starting complex) solution, and decreases with increasing the acid addition (Fig. 1).

The stability constant for $[Co(en)_3]^{2+}$ ($\beta_3 = 10^{13.82}$, in 1 M KCl, Ref. 32, p. 217) is not high enough to prevent its partial dissociation (*c.f.*, that for $[Co(en)_3]^{3+}$: $\beta_3 = 10^{48.69}$, in 1 M KCl, Ref. 32, p. 233). Therefore, $[Co(en)_3]^{2+}$ undergoes stepwise dissociation in accordance with the pattern (*5*), (*6*) or (*7*), depending on the equilibrium concentration of ethanediamine and the value of the $[en]_e/[enH^+]_e$ ratio.

In classical supporting electrolytes, without external addition of acid, it can be assumed that dissociation proceeds *via* $[Co(en)_2(en^*)]^{2+}$ as a very unstable intermediate species, (*5*).

$$[Co(en)_3]^{2+} \underset{k^f_{30^*}}{\overset{k^d_{30^*}}{\rightleftharpoons}} \textit{cis}\text{-}[Co(en)_2(en^*)]^{2+}_{aq} \underset{k^f_{21^*}}{\overset{k^d_{21^*}}{\rightleftharpoons}} \textit{cis}\text{-}[Co(en)_2]^{2+}_{aq} + en \rightleftharpoons \ldots$$

$$\ldots \rightleftharpoons Co^{2+}_{aq} + [Co(OH)_i]^{(2-j)+}_{aq} \qquad (5)$$

The system (*5*), formed at the electrode layer during the first reduction scan, is not totally labile. With insufficient free ethanediamine (when $[[Co(en)_3]^{2+}]_e \ll \sum_0^3 [[Co(en)_i]^{2+}]_e$), its voltammetric oxidation has partly kinetic character. On the other hand, in the ethanediamine solutions with pH ≥ 10, the equilibrium concentration of $[Co(en)_3]^{2+}]$ is practically equal to $\sum_0^3[[Co(en)_i]^{2+}]_e$, and therefore the i_{p_a} value is equal to the i_{p_c} value. Under those conditions, system (*5*) becomes chemically and electrochemically reversible. In consequence, i_{p_a} values (and also i_{p_c}) observed on the cyclic voltammograms for *cis*-$[Co(en)_2(enH)Cl]^{3+}$, $[Co(en)_3]^{3+}$ or $[Co(en)_3]^{2+}$ (as starting complex, respectively) solutions are practically equal to each other.

Hydrogen ion introduction (from a small quantity of strong acid or enH_2X_2 salt; $X = Cl^-$, ClO_4^-) results in acceleration of the dissociation of $[Co(en)_3]^{2+}$. Therefore, a strong decrease of the anodic peak current is observed until its complete decay (curve 2, 3 in Fig. 1). This fact is satisfactorily described by the acid catalysed dissociation mechanism (*6*)

$$\textit{cis}\text{-}[Co(en)_2(enH)]^{3+}_{aq} \underset{k^d_{21}}{\overset{k^d_{21}}{\rightleftharpoons}} \textit{cis}\text{-}[Co(en)_2]^{2+}_{aq} + enH^+ \rightleftharpoons \ldots$$

$$k^+_{21^*}{}^{H} \uparrow\downarrow k^{-H}_{21^*} \qquad (6)$$

$$[Co(en)_3]^{2+} \underset{k^f_{30^*}}{\overset{k^d_{30^*}}{\rightleftharpoons}} \text{cis-}[Co(en)_2(en^*)]^{2+}_{aq} \underset{k^f_{21^*}}{\overset{k^d_{21^*}}{\rightleftharpoons}} \text{cis-}[Co(en)_2]^{2+}_{aq} + en \rightleftharpoons \ldots$$

The acid dissociation pathway was proposed earlier by Shinohara, Lilie and Simic for interpretation of conductometric pulse radiolysis results concerning Co^{2+}-polyamine complexes.[26-27] The contribution of a proton-catalysed pathway increases with increased acid. With a small addition of enH_2^{2+}, *cis*-$[Co(en)_2(enH]^{3+}$ is still unstable and should be regarded as an intermediate species. Similarly, the more mineral acid is added, the more $[Co(en)_2]^{2+}_{aq}$ undergoes stepwise dissociation.

On the other hand, at high concentrations of enH_2Cl_2 or $enH_2(ClO_4)_2$ (≥ 0.5 M) it should be assumed that protonated $[Co(en)_i(enH)]^{3+}_{i=0,1,2}$ complexes coexist with chelated complexes as stable species (*c.f.*, Refs. 41–47). If the above assumption is valid and the $[Co(en)_3]^{2+}$ complex is the electroactive species, and simultaneously, the formation of *cis*-$[Co(en)_2(enH)]^{3+}$ is the rate determining step, and its equilibrium concentration is considerable, then voltammetric oxidation of system (*7*)

$$\begin{array}{l}
[Co(en)_3]^{2+} \underset{k^f_{30*}}{\overset{k^d_{30*}}{\rightleftharpoons}} \text{cis-}[Co(en)_2(en^*)]^{2+}_{aq} \underset{k^{+H}_{11*}}{\overset{k^{+H}_{21*}}{\rightleftharpoons}} \text{cis-}[Co(en)_2(enH)]^{3+}_{aq} \underset{k^f_{21}}{\overset{k^d_{21}}{\rightleftharpoons}} \\
\quad 0.85\text{–}\mathbf{0.77\%} \qquad\qquad\qquad\qquad\qquad\qquad\qquad\qquad\qquad\qquad 22\text{–}\mathbf{63\%} \\
\text{cis-}[Co(en)2]^{2+}_{aq} \underset{k^f_{20*}}{\overset{k^d_{20*}}{\rightleftharpoons}} [Co(en)(en^*)]^{2+}_{aq} \underset{k^{-H}_{11*}}{\overset{k^{+H}_{11*}}{\rightleftharpoons}} [Co(en)(enH)]^{3+}_{aq} \underset{k^f_{11}}{\overset{k^d_{11}}{\rightleftharpoons}} \qquad (7) \\
17\text{–}\mathbf{15\%} \qquad\qquad\qquad\qquad\qquad\qquad\qquad\qquad\qquad\qquad 51\text{–}\mathbf{15\%} \\
[Co(en)]^{2+}_{aq} \underset{k^f_{10*}}{\overset{k^d_{10*}}{\rightleftharpoons}} [Co(en^*)]^{2}_{aq} \underset{k^{-H}_{01*}}{\overset{k^{+H}_{01*}}{\rightleftharpoons}} [Co(enH)]^{3+}_{aq} \underset{k^f_{01}}{\overset{k^d_{01}}{\rightleftharpoons}} Co^{2+}_{aq} \\
\quad 6.3\text{–}\mathbf{6\%} \qquad\qquad\qquad\qquad\qquad\qquad\qquad\qquad\qquad\qquad 3\text{–}\mathbf{0.5\%} \qquad 0.2\text{–}\mathbf{0.18\%}
\end{array}$$

should lead to a considerable increase of anodic peak current, even if the equilibrium concentration of $[Co(en)_3]^{2+}$ is relatively small. The experiment proves the above hypothesis; at $C_{enH_2}(ClO_4)_2 = 2.436$ M pH = 7, one peak (corresponding to electrooxidation of $[Co(en)_3]^{2+}$) is observed (curve 4 in Fig. 1). Under these conditions the i_{p_a}/i_{p_c} value is equal to 0.87, in spite of the small percentage contribution of $[Co(en)_3]^{2+}$ to the total complexation function ($\cong$1% at equilibrium); the basis for the rough evaluation of the percentage distribution of the complexes at equilibrium (scheme (*7*)) is given in Ref. 52. Therefore, at high concentrations of enH_2X_2 (and high values of the $[enH+]_e/[en]_e$ ratio) the rate of reforming of $[Co(en)_3]^{2+}$ increases due to the presence of protonated complexes. The lack of reversible electrodes for the electrometric determination of the equilibrium Co^{2+} concentration and the impossibility of obtaining sufficiently precise values for the potential for the Co^{3+}-en/Co^{2+}-en system (at pH $\leq$ 6) does not allow us to determine the full set of stability constants (including those for $[Co(en)_i(enH)]^{3+}_{i=0,1,2}$).[54] Therefore, on the basis of electrometric data alone, we were unable to calculate a value for the homogeneous rate constant of the rate determining step under conditions represented by schemes (*5*)–(*7*), respectively.

Interpretation of the cyclic voltammetric results in terms of a detailed mechanism for the second step of the reduction in aqueous solution (denoted as (II)/(O) in Fig. 1 and 2) is complicated by the considerable variety of possible species which could take part in the overall electrode process. Complexes existing under those conditions, $[Co^{II}(en)_i(enH^+)_j(H_2O)_{(6-2i-j)}]^{(2+j)+}$, are in fact heterodinuclear species. Therefore, reduction may proceed both *via* Co(II)- and enH^+ groups[55] (for other nitrogen ligands it has been postulated that hydrogen evolution can occur both before and after reduction of the Co(II) centre in the $Co^{(II)}L_nH$ protonated

complex).[56] Irreversible reduction at Co(II) may take place *via* several complex species simultaneously and may involve either two-electron or stepwise one-electron steps (complicated by disproportionation of Co(I) intermediates and regeneration of Co(II) complexes). However, possible intermediates are so unstable that they cannot be identified on the spectroelectrochemical time scale used here. Therefore, we shall limit our discussion to interpretation of results from the equilibrium point of view. It should be noted that even at a high excess of $enH_2(ClO_4)_2$, a new peak is not observed at more positive potentials (in relation to the peak observed for Co(II) in non-complexing, supporting electrolytes). Therefore it is assumed that hydrogen evolution does not proceed before reduction at the Co(II) centre. Other studies show that complexation with ethanediamine (chelate complex formation) stabilizes the second oxidation state and results in two-electron reduction, while the complexation with 2-aminoethylammonium cation (a monodentate ligand) favours the stepwise electrode process.[57] Such behaviour was noted for the Cu(II)-$enH_2(ClO_4)_2$ system, where at high total concentrations of $enH_2(ClO_4)_2$ and low pH values, (stepwise (Cu(II)/Cu(I), Cu(I)/Cu(Hg)) reduction is observed[57] (much smaller degree of wave separation than for Cu(II)-monoamine systems).[58] Under analogous conditions, for the Co(II)-$enH_2(ClO_4)_2$ system, two separate peaks, corresponding to two-step (Co(II)/Co(I), Co(I)/(Co(O)) electrode reduction, are not observed. Therefore, it was assumed that on the voltammetric time scale used in th present study, the electrode reduction occurs at the Co(II) centre, as a two-electron step. The peak current increase with increasing degree of complexation can be explained, assuming that as a result of unstable, intermediate $[Co^{O}(en)_i(enH)_j(H_2O)_{(6-2i-j)}]^{j+}$ product decomposition, the protonated Co(II) complex species is (or are) regenerated at the electrode interface (*via* chemical reaction, — , or alternatively by two charge transfer reactions (first at Co(II) -, secondly on the enH^+ centre) followed by chemical reaction, - - -,), scheme (*8*).

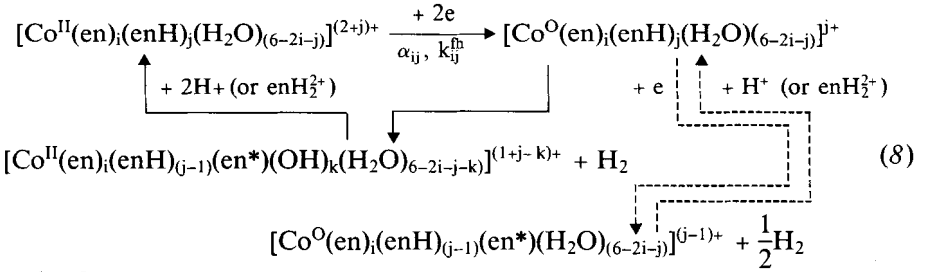

(*8*)

for $j \neq o$, $k = 2$,
$i = j = o$, $k = 2$

Because of the limited range of experimental conditions, it is impossible to distinguish between the two electrode mechanisms. In scheme (*8*) it was assumed that the contribution of the protonated complexes in the observed electrode reaction is privileged, *i.e.* , the heterogeneous standard rate constants and/or charge transfer coefficients are assumed to be greater than for totally chelated complexes. The peak current value is greatest in the domination range of the partly-chelated $[Co(en)_2(enH)]^{3+}$ complex (at nearly neutral pH, curve 4 in Fig. 2). A plausible explanation for this is that the contribution of $[Co(en)_2(enH)]^{3+}$ to the observed electrode reaction, $k_{21}^{fh}\ \beta_{21}\ [en]^2[enH^+]\ \exp\{-\alpha_{21}\ nF/RT(E-E_{21}^{o})\}$, is greater than the

contribution of other, potentially electroactive complexes. On the other hand, at pH ≥5 it is assumed that reduction occurs mainly *via* the Co(II) aquo-cation and $Co(enH)^{3+}$ (curve 1 and 2 in Fig. 2). When $[Co(enH)]^{3+}$, $[Co(en)(enH)]^{3+}$ and $[Co(en)]^{2+}$, $[Co(en)_2]^{2+}$ occur at significant concentrations (i.e., pH ≅ 6, curve 3 in Fig. 2) both protonated complexes are assumed to be electroactive species in the first stage of the overall catalytic process (schem (*8*). Estimation of kinetic parameters for the catalytic process observed in the presence of human blood serum (curve 6 in Fig. 2) is not possible on the basis of electrochemical data alone. Intermediate species are so unstable that they cannot be identified by means of spectroelectrochemical techniques (electronic, ESR) at stationary conditions (even with 0.25 mm – thick thin-layer cells). On the other hand, digital simulation of the broad catalytic peak (curve 6 in Fig. 2) for assumed electroactive species would require an earlier knowledge of the kinetic parameter set $\{k_{ij}^{fh},\alpha_{ij}\}$ for the observed electrode reaction, the full set of stability constants $\{\beta_{ijk}\}$ and homogeneous rate constants for the particular complex formation/dissociation steps $\{k_{ij}^{f},k_{ij}^{d}\}$, as well as considering adsorption parameters. The difficulties in the determination of kinetic parameters result from the complicated character of the observed rate constant of the electrode process, which is the weighted sum of terms, each being the weighted product of thermodynamic (stability constants) and kinetic heterogeneous and homogeneous) parameters and the powers of the respective equilibrium ligand concentrations (*c.f.,* Ref. 42.) Therefore, to solve this problem, further studies are necessary using more selective methods, which would enable, at least partially, independent determination of particular parameters types: thermodynamic (stability constants), kinetic (heterogeneous, homogeneous) and adsorption.

Electrochemistry of cis-[Co(en)$_2$(enH)Cl]Cl$_3$·H$_2$O and [Co(en)$_3$]Cl$_3$ Complexes in DMSO Solution at a Platinum Electrode

Cyclic voltammetric results for *cis*-$[Co(en)_2(enH)Cl]Cl_3 \cdot H_2O$ in 0.1 M TBAP dimethylsulfoxide solution at a platinum working electrode are presented in Figure 3–6 and are summarized in Table 2. In the range 0.3 to – 1.4 V *vs* SCE (satd. NaCl), cyclic voltammetry detects three peaks on the forward half-cycle (at –295, –585 and –1135 mV) and two peaks on the reverse half-cycle (at –518 and 0 mV)

Table 2 Cyclic voltammetric data for $Co(en)_3Cl_3$ and *cis*-$[Co(en)_2(enH)Cl]Cl_3 \cdot H_2O$ at the planar Pt electrode in 0.1 M TBAP – dimethylsulfoxide solution at 25°C.

Complex cation	Medium	Scan rate mV/s	$E_{p_c}^{I}$/mV	$E_{p_c}^{II}$/mV	$E_{p_a}^{II}$/mV	$E_{p_c}^{III}$/mV
cis-$[Co(en)_2(enH)Cl]^{3+}$	0.1 M TBAP/DMSO	200	– 295[a]	– 585.5[b]	– 517.5[b]	– 1135[a]
		100	– 282.5[a]	– 585.5[b]	– 517.5[b]	– 1125.5[a]
		50	– 265[a]	– 585[b]	– 517.5[b]	– 1097.5[a]
		20	– 250[a]	– 585[b]	– 517.5[b]	– 1082.5[a]
				E_{p_c}/mV	E_{p_a}/mV	i_{p_a}/i_{p_c}
$[Co(en)_3]^{3+}$	0.1 M TBAP/DMSO	200		– 585[b]	– 518[b]	0.96
		100		– 585[b]	– 518[b]	0.78
		50		– 585[b]	– 518[b]	0.75
		20		– 585[b]	– 518[b]	0.74

[a] Totally irreversible electrode reaction, [b] Totally reversible electrode reaction, Reference electrode: SCE (satd. NaCl) II 0.1 M TBAP, DMSO.

for a 200 mV s^{-1} scan rate (Fig. 3). It was established coulometrically that the forward half-cycle corresponds to the reduction process. For scan rates lower than 200 mV s^{-1}, on the anodic half-cycle an additional peak is observed (at −280 mV for 100 mV s^{-1} (visible as a shoulder), at −310 mV for 50 mV s^{-1} or at −350 mV for 20 mV s^{-1}), Figure 3. In the range 0.3 to −0.8 V peaks at *ca* 0 mV and −300 mV (on the anodic half-cycle) completely disappear and for all scan rates used only one anodic peak (at −518 mV) was observed (Fig. 3, 4, 6). Consequently, the last peak on the cathodic half-cycle (at −1135 mV) and the last on the anodic half-cycle (*ca* 0 mV, and also at *ca* −300 mV) are coupled peaks (Fig. 3). Similarly, the second cathodic peak (at −585 mV) and the first anodic one (at −518 mV) are coupled peaks (Fig. 3, 4, 6). The first and the third electrode reaction is totally irreversible. The electrochemical irreversibility of the first cathodic peak was confirmed by the linear dependence of the cathodic peak potential, $E^{I}_{p_c}$, *versus* the logarithm of the scan rate (Table 2, Fig. 5). From this dependence, the product of the number of electrons involved in the reduction of *cis*-$[Co(en)_2(enH)Cl]^{3+}$ and the corresponding charge transfer coefficient, $n\alpha = 0.57$, was calculated; assuming n = 1, we obtain $\alpha = 0.57$. Similarly, from the linear dependence of the third cathodic peak potential, $E^{III}_{p_c}$, *versus* the logarithm of the scan rate (Table 2) the $n\alpha$ value 0.53 was obtained. Therefore, the charge transfer coefficient for the second reduction step (Co(II)-en/Co-(0)), is equal to 0.27 (assuming n = 2).

For one cathodic sweep the ratio of the first peak current (corresponding to $[Co(en)_2(enH)Cl]^{3/2+}$ electrode reaction) to the second peak current ($[Co(en)_3]^{3/2+}$) increases with increasing scan rate. On the first cathodic-anodic cycle in the range 0.3 to −0.9 V *vs* SCE and at a sufficiently high scan rate, $v \geq 25$ V s^{-1}, only one peak corresponding to the totally irreversible electrode reaction (*cis*-$[Co(en)_2(enH)Cl]^{3/2+}$) is detected on the cathodic sweep, and no detectable peak on the anodic half-cycle is observed (Fig. 6). At a 25 V s^{-1} scan rate, on the second,

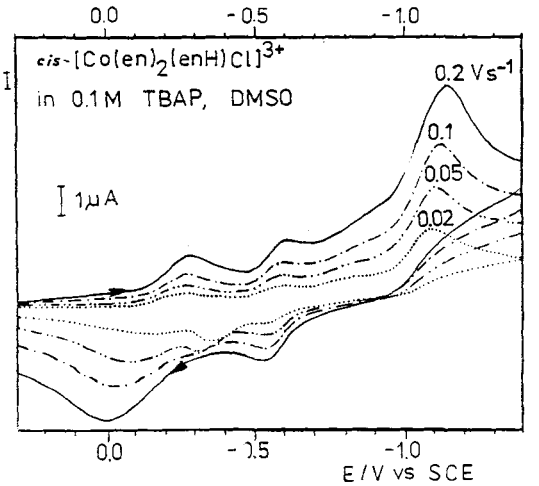

Figure 3 Cyclic voltammograms of $[cis\text{-}[Co(en)_2(enH)Cl]Cl_3 \cdot H_2O]_o = 10^{-3}$ M, $[TBAP]_o = 0.1$ M, DMSO, 25°C, at a platinum electrode. Scan rate: 0.2 V s^{-1} (——), 0.1 V s^{-1} (– – –), 0.05 V s^{-1} (–·–·–) 0.02 V s^{-1} (· · · ·).

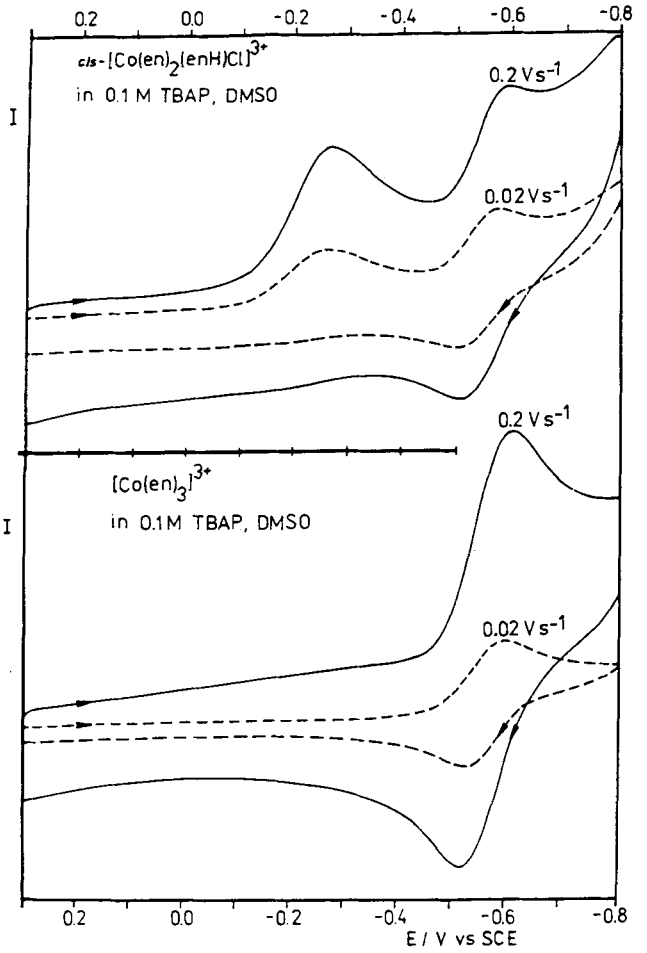

Figure 4 *Upper:* cyclic voltammograms of [*cis*-$[Co(en)_2(enH)Cl]Cl_3H_2O]_o$ = 10^{-3} M, $[TBAP]_o$ = 0.1 M, DMSO, 25°C, at a platinum electrode. Scan rate: 0.2 V s^{-1} (solid line), 0.02 V s^{-1} (dotted line). *Lower:* cyclic voltammograms of $[Co(en)_3^{3+}]_o$ = 10^{-3} M, $[TBAP]_o$ = 0.1 M, DMSO, 25°C, at a platinum electrode. Scan rate: 0.2 V s^{-1} (solid line), 0.02 V s^{-1} (dashed line).

cycle, two peaks, (*cis*-$[Co(en)_2(enH)Cl]^{3/2+}$ and $[Co(en)_3]^{3/2+}$), are observed (on the cathodic half-cycle) and the $[Co(en)_3]^{2/3+}$ peak is detected on the anodic half-cycle. *c.f.*, Fig. 6. On subsequent, cycles the successive decay of the first peak (*cis*-$[Co(en)_2(enH)Cl]^{3/2+}$), the development of the second peak ($[Co(en)_3]^{3/2+}$) on cathodic half-cycles, and the development of the coupled peak ($[Co(en)_3]^{2/3+}$) on anodic half-cycles, are observed. After *ca* twenty cycles, a steady state is reached. Generally, in the steady state the ratio of the second peak current ($[Co(en)_3]^{3/2+}$) to the first peak current ($Co(en)_2(enH)$-$Cl]^{3/2+}$) increases with increase of scan rate. For example, in the steady state obtained when the electrode is cycling between 0.3 and −0.8 V with 0.5 V s^{-1} scan rate, both irreversible (*cis*-$[Co(en)_2(enH)Cl]^{3/2+}$) peak and reversible ($[Co(en)_3]^{3/2+}$, $[Co(en)_3]^{2/3+}$) coupled peaks of comparable height are

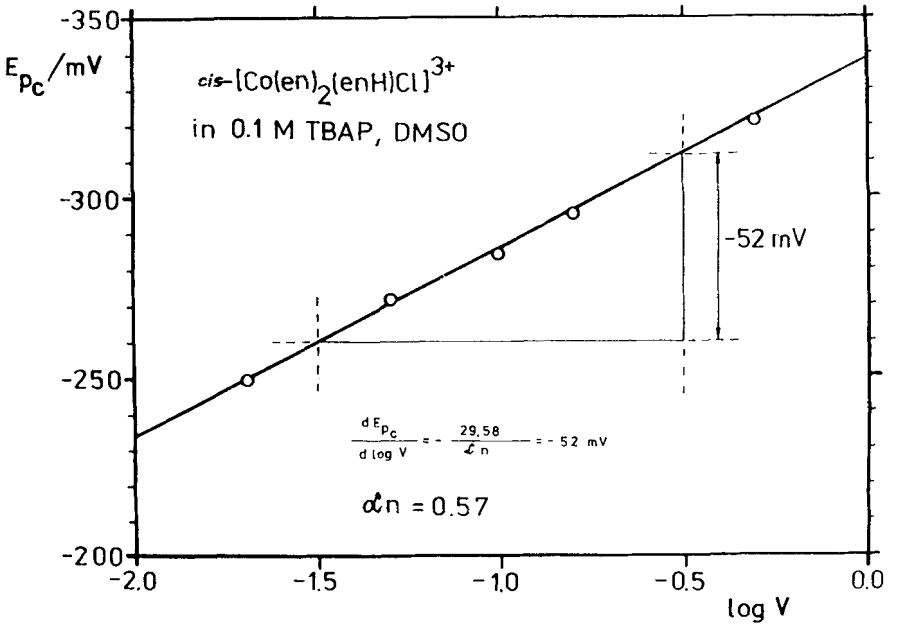

Figure 5 Dependence of cathodic peak potential, E_{p_c}, upon scan rate (log V) for [*cis*-[Co(en)$_2$(enH)Cl]Cl$_3$H$_2$O]$_o$ = 10^{-3} M, [TBAP]$_o$ = 0.1 M, DMSO, 25°C, at a platinum electrode.

observed; for 25 V s^{-1} only the coupled ([Co(en)$_3$]$^{3/2+}$, [Co(en)$_3$]$^{2/3+}$) peaks are detected (Fig. 6). For sufficiently fast repetitive cycling, qualitatively the same steady state voltammogram is obtained independent of whether *cis*-[Co(en)$_2$(enH)Cl]$^{3+}$ or [Co(en)$_3$]$^{3+}$ is used as starting material. However, in the steady state, higher values of cathodic and anodic peak currents are obtained for [Co(en)$_3$]$^{3+}$ as starting complex than for *cis*-[Co(en)$_3$(enH)Cl]$^{3+}$ at the same total concentration (without external en addition).

Rationalization of the Electrochemical Results for cis-[Co(en)$_2$(enH)Cl]Cl$_3$·H$_2$O and [Co(en)$_3$]Cl$_3$ in DMSO Solution at a Platinum Electrode

In DMSO, at the platinum electrode, the voltammetric peak observed corresponds directly to the reduction of *cis*-[Co(en)$_2$(enH)Cl]$^{3+}$. That is a basic difference between the voltammograms obtained for *cis*-[Co(en)$_2$(enH)Cl]$^{3+}$ at platinum in DMSO and at mercury electrodes in aqueous solution.

The one-electron, irreversible reduction of *cis*-[Co(en)$_2$(enH)-Cl]$^{3+}$ is the first step ($\vec{E}$-1) of the overall electrode process, as follows.

$$\text{cis-[Co(en)}_2\text{(enH)Cl]}^{3+} + e \xrightarrow{\alpha_{211}, k_{211}^{fh}} \text{cis-[Co(en)}_2\text{(enH)Cl]}^{2+} \qquad (\vec{E}\text{-}1)$$

For sufficiently fast scan rates ($v \geq 25$ V s^{-1}), the overall electrode process becomes the single step ($\vec{E}$-1), *c.f.*, Fig. 6). Under these conditions the cathodic charge transfer coefficient, α_{211} = 0.57, and the corresponding heterogeneous rate constant, k_{211}^{fh} = $8 \cdot 10^{-6}$ cm s^{-1} were estimated.[59]

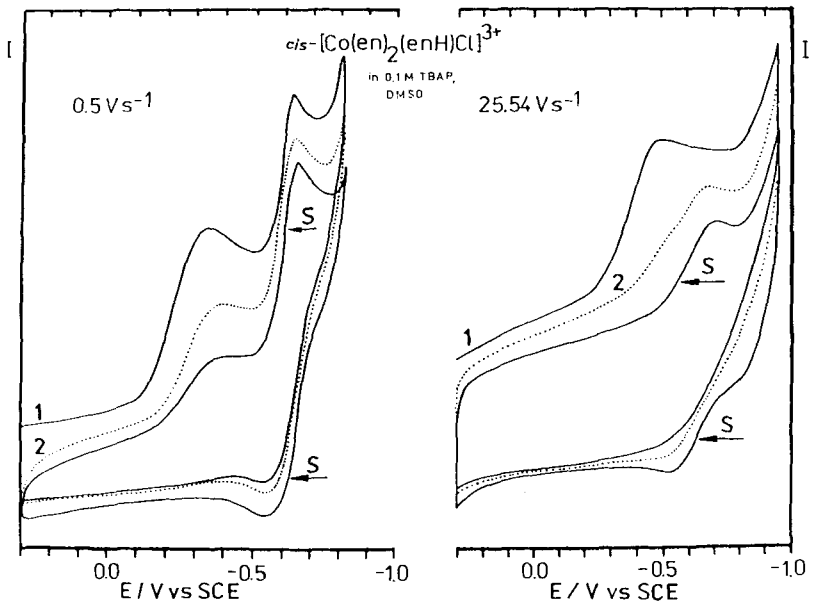

Figure 6 Repetitive cyclic voltammograms of $[cis\text{-}[Co(en)_2(enH)Cl]Cl_3 \cdot H_2O]_o = 10^{-3}$ M, $[TBAP]_o = 0.1$ M, DMSO, 25°C, at a platinum electrode. Scan rate = 0.5 V s^{-1} (*left figure*), 25 V $\cdot s^{-1}$ (*right figure*); (1)-first cycle (solid line), (2) – second cycle (dotted line), (S) – steady state (solid line).

DMSO is an aprotic solvent of high donor number (*ca* 30)[60], strongly interacting with cations. Stability constants for ethanediamine complexes in DMSO are much greater than for their analogues in aqueous solution ($\beta_2^{DMSO}/\beta_2^{H_2O} = 10^3$, for $[M(en)_2]^{2+}$, $\beta_3^{DMSO}/\beta_3^{H_2O} = 10^5$, for $[M(en)_3]^{2+}$)[61]. Values are available only for M = Zn^{2+}, Cd^{2+} (Ref. 61); for Co^{2+} values of respective stability constants should be of the same order of magnitude (*c.f.*, Ref. 62). It can be assumed, therefore, that the protonated and chelated ethanediamine Co(II) complexes should be thermodynamically more stable in DMSO than in aqueous solutions. Kinetically, however, the Co(II)-ethanediamine complexes are relatively labile species in both solvents. For slow scan rates ($v < 25$ V s^{-1}), an ECE-type electrode process is observed. Under these conditions the chemical step (*9*) is the resultant of two opposing tendencies: dissociation, *cis*-$[Co(en)_2(en^*)]^{2+} \rightarrow [Co(en)_2]^{2+}$, and chelate ring closure, (*cis*-$[Co(en)_2(en^*)]^{2+} \rightarrow [Co(en)_3]^{2+}$).

$$\text{cis-}[Co(en)_2(enH)Cl]^{2+} \underset{k_{211}^{+Cl^-}}{\overset{k_{211}^{-Cl^-}}{\rightleftharpoons}} \text{cis-}[Co(en)_2(enH)]^{3+} + Cl^- \qquad (9)$$
$$+ S$$

$$k_{21^*}^{-H} \uparrow\downarrow k_{21^*}^{+H}$$

$$[Co(en)_3]^{2+} \underset{k_{30^*}^{d}}{\overset{k_{30^*}^{f}}{\rightleftharpoons}} \text{cis-}[Co(en)_2(en^*)]^{2+} \underset{k_{21^*}^{f}}{\overset{k_{21^*}^{d}}{\rightleftharpoons}} [Co(en)_2]^{2+} \rightleftharpoons \ldots$$
$$+ SH^+$$

Here, SH^+ denotes the solvated proton. Among the complexes formed in the electrode layer, only $[Co(en)_3]^{2+}$ is electroactive as far as reversible electrooxidation

is concerned.[63] Moreover, $[Co(en)_3]^{2+}$ oxidizes reversibly to $[Co(en)_3]^{3+}$ species, ($\vec{E}$-2), (*4*)), in the potential range at which the starting *cis*-$[Co(en)_2(enH)Cl]^{3+}$ complex undergoes totally irreversible reduction (Fig. 3, 4, 6).

For the system studied here, in the potential range, $E_{1/2}^{irrev}$ ($\vec{E}$-1) < E $E_{1/2}^{rev}$-($\vec{E}$-2), current decrease to negative values is not observed during the first cathodic half-cycle even at very slow scan rates (5 mV s^{-1}). Therefore, we can neither confirm nor exclude the contribution of homogeneous disproportionation (*10*) in the observed electrode process,

$$cis\text{-}[Co(en)_2(enH)Cl]^{3+} + [Co(en)_3]^{2+} \rightleftharpoons cis\text{-}[Co(en)_2(enH)Cl]^{2+} + [Co(en)_3]^{3+}$$
$$\uparrow\downarrow$$
$$\sum_{i=0}^{i=N}\sum_{j=0}^{j=1}\sum_{k=0}^{k=1}[Co(en)_i(enH)_j(Cl)_k]^{(2+j-k)+}, \qquad (10)$$

Here, N≤3,
on the basis of Feldberg's and Jeftic's[64] and Gosser's and Rieger's[65] theoretical treatment and simulations of the $\vec{E}\vec{C}\vec{E}$ mechanism.

The mechanism of the redox cross reaction (outer-sphere, (10), or inner-sphere, (12) cannot be solved on the basis of voltammetric data alone. If we take into account the fact that $[Co(en)_3]^{2+}$ is formed (in the electrode layer) from the partly chelated intermediate species *cis*-$[Co(en)_2(en^*)]^{2+}$, and that the equilibrium (*11*) exists,

$$[Co(en)_3]^{3+} \underset{k^d_{30^*}}{\overset{k^d_{30^*}}{\rightleftharpoons}} [Co(en)_2(en^*)]^{3+};\ K_T = \frac{k^f_{30^*}}{k^d_{30^*}} = \frac{[Co(en)_3]^{3+}}{[Co(en)_2(en^*)]^{3+}}, \qquad (11)$$

we cannot exclude, *a priori*, the formation of a short-lived, Cl^--bridged, intermediate species (*12*). Consequently, the redox cross-reaction according to the inner-sphere mechanism (*12*) cannot be excluded.

$$cis\text{-}[Co^{III}(en)_2(enH)Cl]^{3+} + [Co^{II}(en)_2(en^*)]^{2+} \rightleftharpoons$$
$$\rightleftharpoons \left[(en)_2Co^{III}\underset{\underset{enH^+}{|}}{}Cl\underset{\underset{en^*}{|}}{}Co^{II}(en)_2\right]^{5+} \rightleftharpoons \qquad (12)$$
$$\rightleftharpoons cis\text{-}[Co^{II}(en)_2(enH)Cl]^{2+} + [Co^{III}(en)_3]^{3+}$$
$$\uparrow\downarrow$$
$$\sum_{i=0}^{i=N}\sum_{j=0}^{j=1}\sum_{k=0}^{k=1}[Co^{II}(en)_i(enH)_j(Cl)_k]^{(2+j-k)+},$$

Separate kinetic studies are now in progress to make clear the possible contribution of the redox cross reaction in the overall $\vec{E}\vec{C}\vec{E}$-type electrode process.

The present data demonstrate that not only $[Co(en)_3]^{3+}$ but also *cis*-$[Co(en)_2(enH)Cl]^{3+}$ is an electrode active species. Dynamic electrochemistry reveals that the electrochemical conversion of *cis*-$[Co(en)_2(enH)Cl]^{3+}$ complex cation (as starting compound) to $[Co(en)_3]^{3+}$ proceeds according to the $\vec{E}\vec{C}\vec{E}$ mechanism. The first electrochemical step (*cis*-$[Co(en)_2(enH)Cl]^{3/2+}$ ($\vec{E}$-1)) is irreversible. In the chemical stage (the ring closure step) labile $[Co(en)_3]^{2+}$ is formed. This process is the result of two opposing tendencies: (i) for dissociation,

cis-$[Co(en)_2(en^*)]^{2+} \rightleftharpoons [Co(en)_2]^{2+}$ + en, or *cis*-$[Co(en)_2(enH)]^{3+} \rightleftharpoons [Co(en)_2]^{2+}$ + enH^+ (in the acid media), and (ii) for chelate ring closure, *cis*-$[Co(en)_2(en^*)]^{2+} \rightleftharpoons [Co(en)_3]^{2+}$. In the second electrochemical step ($[Co(en)_3]^{2/3+}$) the heterogeneous electron transfer reaction is fast. In DMSO, both electrochemical stages are observable, while in H_2O only the second ((E-2), (*4*)) is directly observed.

DC polarographic (at DME) and voltammetric (at HMDE) reduction of the Co(II)-en system is characterized by variation in the electrode reaction mechanism with change of complexation degree. For the Co(II)-en/enH^+-human blood serum system, only one, broad, catalytic peak is observed (probably a mixture of several strongly overlapping peaks). This fact differentiates the corresponding diamine and monoamine-Co(II)-blood serum systems (in the latter system, three, well-separated peaks are detected).

The present data allow qualitative recognition of the electrode reaction mechanism. However, for estimation of electrode and chemical kinetic parameters for the electrometrically induced convertion of *cis*-$[Co(en)_2(enH)Cl]^{3+}$ to $[Co(en)_3]^{3+}$, and for quantitative description of variation in electrode reaction mechanism with changes of complexation degree in the absence of the human blood serum (and of the catalytic process observed in the presence of the human blood serum), further fast scan electrochemical and spectroscopic investigations would naturally be required.

Acknowledgements

This work was supported by the Committee for Scientific Research (Poland) under grant No KBN 207359101.

References

1. S.M. Jørgensen, *J. Prakt. Chem.*, **39**, 1 (1889).
2. A. Werner, unpublished manuscript dated June 1916, see: G.B. Kauffman, *Inorg. Chem.*, **7**, 1694 (1968).
3. H.D.K. Drew, F.W. Pinkard, G.H. Preston and W. Wardlaw, *J. Chem. Soc.*, 1895 (1932).
4. H.D.K. Drew, *J. Chem. Soc.*, 2338 (1932).
5. H.D.K. Drew and N.H. Pratt, *J. Chem. Soc.*, 506, (1937).
6. G. Schwarzenbach and B. Magyar, *Helv. Chim. Acta*, **45**, 1454 (1962).
7. M.D. Alexander and C.A. Spillert, *Inorg. Chem.*, **9**, 2344 (1970).
8. J.A. Olabe and P.J. Aymonino. *J. Inorg. Nucl. Chem.*, **36**, 1221 (1974).
9. J.D. Petersen and F.P. Jakse, *Inorg. Chem.*, **16**, 2845 (1977).
10. T. Matsubara and P.C. Ford, *Inorg. Chem.*, **17**, 1747 (1978).
11. B.S. Rasmussen and F. Galsbøl, XXII I.C.C.C., Budapest, Hungary, August 23–27, 1982, Abstracts of Papers, Vol. 2, p. 666; F. Galsbøl and B.S. Rasmussen, *Acta Chem. Scand.*, **36**, 439 (1982).
12. F.P. Fanizzi and G. Natile, *J. Chem. Soc., Dalton Trans.*, 1467 (1984).
13. G. Natile and F.P. Fanizzi, *J. Chem. Soc., Dalton Trans.*, 1057 (1985).
14. F. Galsbøl, T. Glowiak, A. Hammershøi, B.S. Hammershoi, S. Larsen and M. Wilgocki, *Acta Chem. Scand.*, **44**, 31 (1990).
15. H.L. Schläfer and R. Kling, *Z. Phys. Chem., Neue Folge (Frankfurt am Main)*, **16**, 14 (1958).
16. E. Jørgensen and J. Bjerrum, *Acta Chem. Scand.*, **13**, 2075 (1959).
17. W. Kruse and H. Taube, *J. Am. Chem. Soc.*, **83**, 1280 (1961).

18. O. Mønsted and J. Bjerrum, Det. 13 Nordiske Kemiker møde i København, August 1968, p. 60; XI I.C.C.C., Haifa and Jerusalem, September 1968, Proceedings, (Elsevier, Amsterdam, 1968), p. 108.
19. R.F. Childers, Jr., K.G. Van der Zyl, Jr., D.A. House, R.G. Hughers and C.S. Garner, *Inorg. Chem.*, **7**, 749 (1968).
20. W. Geis and H.L. Schläfer, Z. *Phys. Chem., Neue Folge (Frankfurt am Main)*, **65**, 107 (1969).
21. S.C. Pyke and R.G. Linck, *Inorg. Chem.*, **10**, 2445 (1971).
22. C. Bifano and R.G. Linck, *Inorg. Chem.*, **13**, 609 (1974).
23. L. Mønsted and O. Mønsted, *Acta Chem. Scand.*, **29**, 29 (1975).
24. P. Andersen, T. Berg and J. Jacobsen, *Acta Chem. Scand.*, **29**, 381 (1975).
25. L. Mønsted, *Acta Chem. Scand.*, **30**, 599 (1976).
26. J. Lilie, N. Shinohara and M.G. Simic, *J. Am. Chem. Soc.*, **98**, 6516 (1976).
27. N. Shinohara, J. Lilie and M.G. Simic, *Inorg. Chem.*, **16**, 2809 (1977).
28. C.F.C. Wong and A.D. Kirk, *Inorg. Chem.*, **16**, 3148 (1977).
29. R.A. Read and D.W. Margerum, *Inorg. Chem.*, **20**, 3143 (1981).
30. H.E. Toma and N.Y.M. Iha, *Inorg. Chem.*, **21**, 3573 (1982).
31. R.A. Read and D.W. Margerum, *Inorg. Chem.*, **22**, 3447 (1983).
32. J. Bjerrum, "Metal Ammine Formation in Aqueous Solution" (P. Haase and Son, Copenhagen 1941), reprinted 1957.
33. H.A. Laitinen, P. Kivalo, *J. Am. Chem. Soc.*, **75**, 2198 (1953); P. Kivalo, *J. Am. Chem. Soc.*, **77**, 2678 (1955).
34. J. Dolezal, *Chem. Listy*, **49**, 1237 (1955); *Coll. Czechoslov. Chem. Commun.*, **21**, 113 (1956).
35. D. Konrad and A.A. Vlček, *Coll. Czechoslov. Chem. Commun.*, **28**, 808 (1963); see also, *ibid.*, **28**, 595 (1968).
36. M. Ito, *Nippon Nogei – Kagaku Kaishi*, **32**, 201 (1958); *Chem. Abstracts*, **53**, 2884d (1959).
37. H. Bartelt and H. Skilandat, *J. Electroanal. Chem.*, **23**, 407 (1969).
38. J.J. Ibanez, C.S. Choi and R.S. Becker, *J. Electrochem. Soc.*, **134**, 3083 (1987).
39. H. Ogino, *J. Coord. Chem.*, **15**, 187 (1987).
40. E. Fischerova, O. Dračka and M. Meloun, *Coll. Czechoslov. Chem. Comm.*, **33**, 473 (1968).
41. J. Biernat and M. Wilgocki, *Roczniki Chem.*, **48**, 1663 (1974); *ibid.*, **51**, 1305 (1977).
42. M. Wilgocki, 'Polarographic Determination of Stability Constants for Chelate and Partly-Chelate as well as Non-chelate Metal-ion Complexes with Bidentate Ligands', (Wroclaw University Press, Wroclaw, 1982).
43. M. Wilgocki and J. Bjerrum, *Acta Chem. Scand.*, **37**, 307 (1983).
44. M. Wilgocki, *J. Coord. Chem.*, **14**, 39, 151 (1985).
45. M. Wilgocki, *J. Coord. Chem.*, **16**, 357 (1988).
46. M. Wilgocki, *J. Coord. Chem.*, **18**, 263, 369 (1988).
47. M. Wilgocki, *J. Coord. Chem.*, **28**, 51 (1993).
48. J.B. Work and J. Mc Reynolds, *Inorganic Syntheses, II*, 221 (1946).
49. V. Alexeyev, 'Quantitative Analysis', (Mir Publishers, Moscow, 1969), p. 413.
50. M. Wilgocki, T. Szymańska-Buzar, M. Jaroszewski and J. Ziółkowski, Proc. 2nd Beijing Conf. and Exhib. on Instrum. Analysis, 1229 (1987); M. Moszner, M. Wilgocki and J. Ziółkowski, *J. Coord. Chem.*, **20**, 219 (1989).
51. J. Heyrovsky and J. Kuta, 'Principles of Polarography', (Mir Publishers, Moscow, 1965), pp. 395–400, and references therein.
52. The Co^{2+}-, Cd^{2+}- and Zn^{2+}- en systems show great similarity. Knowing stability constants for the chelate complexes of Co^{2+} (Ref. 32, p. 217), Cd^{2+} and Zn^{2+} (Ref. 53) as well as for protonated complexes of Cd^{2+} (Ref. 43), Zn^{2+} (Ref. 44) with ethanediamine, and for Co^{2+} (Ref. 32, p. 187), Cd^{2+} and Zn^{2+} complexes (Ref. 32, p. 162) with ammonia, stability constants were roughly estimated for $[Co(en)_i(enH)]^{3+}{}_{i=0,1,2}$ complexes (as in Ref. 43). For this, it was assumed that: (i) the stability constant for $Co(enH)^{3+}$ should be not greater than β_{01} ($= 10^{1.7}$) for $Cd(enH)^{3+}$ and not smaller than $\beta_1^{Co(NH_3)^{2+}}/\beta_{01}^{Cd(enH)^{3+}}$ ($= 10$); (ii) while estimating β_{11} for $[Co(en)(enH)]^{3+}$ it was assumed that $1.0 \leq \log(\beta_{11}/\beta_{10}) \leq 1.5$, while for $[Co(en)_2(enH)]^{3+}$, $0.7 \leq \log(\beta_{21}/\beta_{20}) \leq 1.0$. Finally, the calculations (scheme (7)) were carried out with: $\log\beta_{01}$ = **1.0**–1.7, $\log\beta_{10}$ = 5.89 (Ref. 32, p. 217), $\log\beta_{11}$ = **6.89**–7.39,, $\log\beta_{20}$ = 10.72 (Ref. 32, p. 217.), $\log\beta_{21}$ = 11.42–**11.92**, $\log\beta_{30}$ = 13.82 (Ref. 32, p. 217), using $\log k_1^H$ = 10.81, $\log k_{12}^H$ = 7.93 as protonation constans of ethanediamine.[43]
53. J. Bjerrum an P. Andersen, *Kgl. Danske Vidensk., Matt.-Fys. Medd.*, **22**, 1 (1945).

54. As with the Cd^{2+}- and Zn^{2+}-en system,[43,44] a strong overlapping of the contributions resulting from equilibrium concentrations of protonated and chelated complexes can also be expected for the Co^{2+}-en system. Therefore, stability constants for all complexes coexisting in equilibrium should be determined simultaneously. This, in turn, would require measurements in the $3 \leq pH \leq 8$ range. For $pH<6$, equilibrium at the platinum electrode is not established in Co(III)-/Co(II)-en solutions, a fact which excludes the use of the redox titration method.
55. The acid properties of the protonated complexes decline the series: $Co(enH)^{3+} > Co(en)(enH)^{3+} > enH_2^{2+} > Co(en)_2(enH)^{3+} >> enH^+$ (estimated with stability constants roughly evaluated in Ref. 52 and acid dissociation constants of enH_2^{2+}, enH^+ determined in Ref. 43).
56. V.F. Toropowa G.K. Budnikow and E.P. Mediantseva, in 'Polarography, Problems and Perspectives' (in Russan), J.P. Stradin and S.G. Majranovskij (Eds), (Zinante, Riga, 1977), p. 224–225, and references therein.
57. M. Wilgocki, unpublished results.
58. D.R. Crow, 'Polarography of Metal Complexes', (Academic Press, London, 1969), pp. 77–80.
59. Since the value of the formal potential (E_f°) for the $\vec{E}$-1 electrode reaction is not known, the k_{211}^{fh} value was estimated with $E_f^\circ = 0$ (*versus* SCE; satd. NaCl). If the formal potential for *cis*-$[Co(en)_2(enH)Cl]^{3+}$ complex becomes available, the value of the standard heterogeneous electrode reaction ($\vec{E}$-1) rate constant can be estimated from $\log k_s = \log k_{211}^{fh} - (\alpha/0.059)E_f^\circ$.
60. V. Gutmann, 'Coordination Chemistry in Non-Aqueous Solutions', (Springer-Verlag, Wien, 1968), p. 155; *Topics in Current Chemistry,* **27,** 59 (1972).
61. K.H. Pool and D.H. Sandberg, *Talanta,* **16,** 1319 (1969).
62. R.M. Smith, A.E. Martell and R.J. Motekaitis, 'NIST Critical Stability of Metal Complexes Database', (U.S. Department of Commerce National Institute of Standards and Technology, Standard Reference Data Program, Gaithersburg, 1993).
63. All complexes of formula $[Co(en)_i(enH)_j]^{(2+j)+}$, can undergo totally irreversible reduction with individual rates, $k_{ij}^{fh}\ \beta_{ij}\ [en]^i[enH^+]^j\ \exp\{-\alpha_{ij}nF/RT(E-E_{ij}^\circ)\}/\Sigma\beta_{ij}[en]^i[enH]^j$, at a more negative potential range according to parallel charge transfer mechanism, but only $[Co(en)_3]^{2+}$ can undergo a totally reversible oxidation.
64. S.W. Feldberg and L. Jeftic, *J. Phys. Chem.,* **76,** 2439 (1972).
65. D.K. Gosser and P.H. Rieger, *Anal. Chem.,* **60,** 1159 (1988).